

Entropic sampling of star-shaped polymers with different number of arms: temperature dependencies of structural properties

I. A. Silanteva¹, P. N. Vorontsov-Velyaminov¹

¹Saint Petersburg State University, Dept. of molecular biophysics and polymer physics,
Faculty of Physics, 198504, Saint Petersburg, Russia
sila3@yandex.ru, voron.wgroup@gmail.com

PACS 02.70.-c, 02.70.Uu, 05.10.Ln, 05.70.-a, 05.70.Fh, 07.05.Tp, 36.20.-r, 36.20.Hb, 64.60.-i, 64.70.Nd, 64.70.km, 64.70.pj, 65.40.Ba, 65.80.+n, 81.07.Nb, 82.20.Wt, 82.35.Lr, 87.10.Rt, 87.15.ak, 87.16.aj, 87.53.Wz, 87.55.K

DOI 10.17586/2220-8054-2015-6-4-513-523

The lattice model for a star-shaped polymer with a total number of up to 72 segments is considered. The number of arms varied, ranging from 2 to 6. Entropic sampling Monte Carlo simulation is used to obtain the equilibrium, thermal and structural properties of the considered systems over a wide range of temperatures. The coil-globule transition is observed and the transition temperature is shown to shift toward lower temperatures with an increase in the number of arms. This study demonstrates how the structure of the star-shaped polymer affects its equilibrium properties.

Keywords: star-shape polymer, lattice model, entropic sampling, Wang-Landau algorithm, phase transition.

Received: 20 June 2015

1. Introduction

Over the last couple of decades, there has been an increased interest in studying nano-objects of various types including the polymer molecules. Modern facilities are now able to synthesize macromolecules with complicated architecture, such as stars, brushes, nets or dendrimers. In this paper, we restrict ourselves to the simulation study of star-shaped molecules. Due to their specific structural features, these polymers have essentially new characteristics in comparison to linear chains. As a result, their average size is considerably smaller than that of the linear polymers with the same number of segments. Consequently, they have greater concentration of monomers that leads to greater volume effects. Star-like molecules can be considered as unique objects, combining properties of linear polymers and colloid particles as was also pointed out in [1, 2]. It was correctly mentioned in [3] that the star polymer with a small number of arms is close in its behavior and properties to that of a linear polymer, while with an increased number of arms, it becomes closer to a rigid spherical particle. The main aim of this paper is to observe how initial structural characteristics, such as the number of its arms, influence its equilibrium structural properties, including features of the coil-globule transition. This problem is also discussed in a number of papers [4, 5] so it would be desirable to compare our data with that of [4]. It is known that in the star-like polymers, there can be observed transitions of two types: liquid-crystal (1st order) and the coil-globule (2nd order), wherein the second order transition is very sensitive to the polymer's topology.

It should also be stressed that studies of star-like polymers are important because of their possible application for the transport of DNA and drug substances into cells [6–8].

The considered model is presented in section 2. The results for the athermal and thermal cases are discussed in sections 3 and 4 correspondingly. Conclusions are given in section 5.

2. Model

In this work, we consider the model of a regular neutral polymer star on a simple cubic (SC) lattice. Lattice models have been widely used for a long time in the study of polymers [9]. These models are still useful now [10–14], since such an approach allows one to obtain reasonable results with minimal computational requirements.

Star-like polymers (for convenience, we refer to as "star") can be represented as f chains fixed by their single ends to a common center. We consider cases of $f \leq 6$ where $f=1$ and $f=2$ correspond to linear chains. Each arm is a chain of N_{arm} bonds (segments) and $N_{\text{arm}} + 1$ monomers (knots). The total number of segments in a star is $N = fN_{\text{arm}}$. Each i -th monomer has coordinates (x_i, y_i, z_i) . The segments are being generated with the aid of semi-phantom random walks along the lattice with reverse steps being forbidden [15], contrary to the case of free (or phantom) walks. In order to change the configuration of the star, an arm and its k_0 -th monomer are randomly chosen and a new piece of this arm, starting from k_0 up to the end of the arm, is newly generated.

In our work, we use the entropic sampling simulations [16, 17] within Wang-Landau algorithm [18]. This method was successfully applied in our previous works [13, 15, 19–21] as well as by other authors [4, 12, 22–24] in polymer studies. An important attractive feature of this method is in its ability to obtain statistics for very rare events with relative ease. Hence, this method provides a means for calculating the equilibrium characteristics of the studied system over a wide range of temperatures, including the phase transition area. The calculation time required was about a few hours on a standard 4-core processor in most instances.

3. Athermal case

In the athermal case, the interaction between monomers is reduced to the exclusion of intersections. In order to learn how strongly the fixation of all arms' ends at the same point (in the center of the star) restricts their freedom, it is worth considering their excess entropy. The complete number of conformations for a semi-phantom star with $f \leq z$ arms is $z!(z-1)^{N-f}/(z-f)!$ [21]. So, the entropy can be expressed as:

$$S = \ln \left(\frac{z!(z-1)^{N-f}}{(z-f)!} \Omega_0 \right), \quad (1)$$

where $z=6$ is the coordinate number of our SC lattice and Ω_0 is the ratio of the self-avoiding conformations which we obtain in the same way as in our preceding paper [21]. Values of Ω_0 were calculated for stars with the total number of segments $N \leq 800$. The error does not exceed 15%. The entropy of the phantom chain (star) is $\ln(z^N)$. So the specific excess entropy of our system (relative to this basic system) is:

$$\frac{\Delta S}{N} = \frac{1}{N} \ln \left(\frac{z!(z-1)^{N-f}}{(z-f)!} \Omega_0 \right) - \ln z. \quad (2)$$

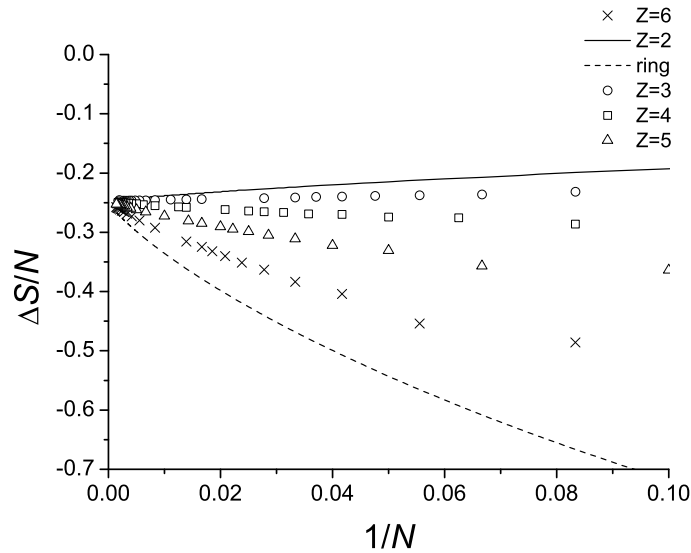


FIG. 1. Specific excess entropy (relative to the phantom chain) as a function of the inverse number of segments for stars with different numbers of arms ($3 \div 6$), for a chain, and for ring [15].

The dependence of $\Delta S/N$ on $1/N$ is presented in Fig. 1. It is seen that for the 3-arm star, the curve in this scale is rising and is rather close to that of the single chain. But for $f=4$, the dependency already begins to decrease; and with an increased number of arms, this tendency becomes more pronounced. This picture demonstrates that increasing the number of arms results in increased configurational restrictions. For comparison, Fig. 1 presents the appropriate curve for ring chains [15] and it is seen that restrictions caused by closure of the chain are even greater than in the case of when the 6 arms were affixed to the center of the star.

4. Thermal case

In the thermal case, we account also for interactions of non-bonded monomers if they occur in contact with each other (i.e. at a distance of the lattice constant). In this case, an energy ($\epsilon > 0$ or $\epsilon < 0$) is attributed to each such contact. The value of ϵ can characterize the solvent quality of the real polymer solutions. In this work, we present only the most interesting case — attraction ($\epsilon < 0$). The energy in the given conformation is $E = \epsilon m$, where m is the number of contacts, $m \in [0, m_{\max}]$. As a result of the simulation for a given star, we obtain a distribution of conformations over the number of contacts Ω_m for a given star. Knowledge of Ω_m allows calculation of equilibrium properties over a wide temperature range, according to the canonical expression:

$$\langle F \rangle (T) = \frac{\sum_{m=0}^{m_{\max}} F_m e^{-E_m/k_B T} \Omega_m}{\sum_{m=0}^{m_{\max}} e^{-E_m/k_B T} \Omega_m}, \quad (3)$$

where F is a certain physical quantity and F_m is its distribution over the number of contacts which is also determined during simulation. In this paper, we obtained such distributions for

the module of the radius-vector of the center of mass, mean square of the radius of gyration and its orthogonal components. In the limit $T \rightarrow \infty$, equation (3) yields the athermal values.

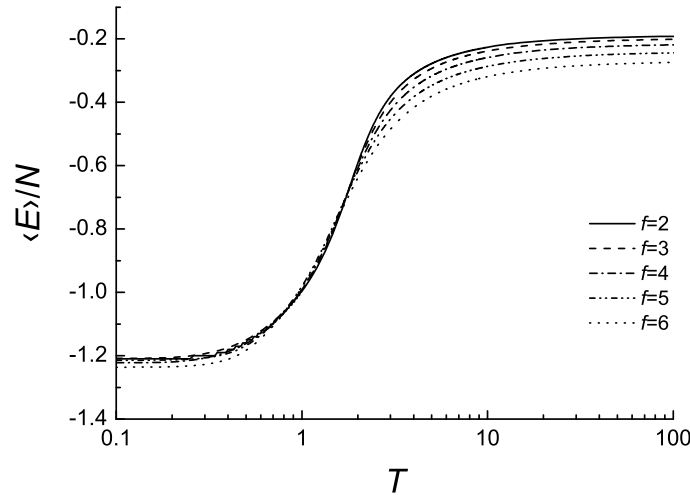


FIG. 2. Specific configuration energy as a function of temperature for stars with different numbers of arms (3 ÷ 6) and for a chain. Total number of segments $N=70$ for $f=5$ and $N=72$ for all the rest.

We have studied stars with different numbers of arms (from 3 to 6) and approximately equal total number of segments: $f=3$, $N_{\text{arm}}=24$; $f=4$, $N_{\text{arm}}=18$; $f=5$, $N_{\text{arm}}=14$; $f=6$, $N_{\text{arm}}=12$. Also, for comparison, the chain (i.e. $f=2$, $N_{\text{arm}}=36$) has been considered. The case with a fixed number of arms ($f=6$) was studied earlier in [19–21]. Fig. 2 presents temperature dependencies of the specific configuration energy according to (3) with $F_m = \epsilon m$. Here and subsequently, the temperature is given in $|\epsilon|$ -units, $k_B T / |\epsilon|$. A monotonic growth of the energy was observed, with the curves being close to each other and a very small difference between them is only noticeable at higher temperatures.

In order to observe structural transitions, it is also useful to calculate the heat capacity:

$$C(T) = \frac{\partial E}{\partial T} = \frac{\langle E^2 \rangle (T) - (\langle E \rangle (T))^2}{T^2}. \quad (4)$$

The temperature dependence of the specific heat capacity is presented in Fig. 3. It was observed that for all the considered cases, there exists a maximum which becomes wider and is shifted to lower temperatures with an increased number of arms. The latter provides the increase of the total monomer density, such that it hinders the collapse of the coil-globule transition. Similar results were obtained in [4], where the fluctuating bond model was used.

Additionally, we present several structural characteristics for our models. In order to observe the coil-globule structure transition, we calculated the mean square radius of gyration for a star. For each conformation, the radius of gyration was determined and was ultimately averaged separately for each number of contacts using the following equation:

$$\langle R_g^2 \rangle_m = \frac{1}{2N^2} \left\langle \sum_{i=1}^N \sum_{j=1}^N |r_{ij}|^2 \right\rangle_m = \frac{1}{N} \left\langle \sum_{i=1}^N (r_i - R_c)^2 \right\rangle_m. \quad (5)$$

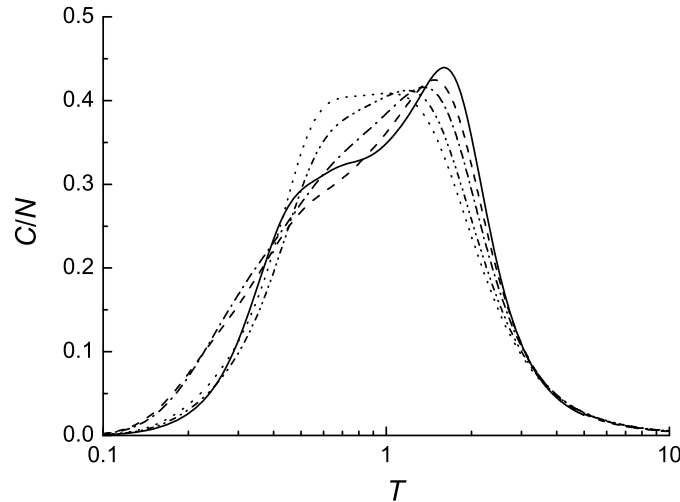


FIG. 3. Specific heat capacity as a function of temperature for stars with different numbers of arms ($3 \div 6$) and for a chain. $N=70$ for $f=5$ and $N=72$ for all the rest. Legend, see in Fig. 2.

Here, r_{ij} is the distance between monomers and the sum is taken over all monomeric pairs, R_c is the center of mass vector. The obtained data is canonically averaged according to formula (3). The dependence of the mean square radius of gyration on temperature is shown in Fig. 4a. In Fig. 4b data is presented for the T -dependence of the factor $g = \langle R_I^2 \rangle_{\text{star}} / \langle R_I^2 \rangle_{\text{chain}}$. The latter is shown to be non-monotonic and there exists a temperature at which the star attains the most extended state in comparison with that of the corresponding chain. At higher temperatures, for increasing f , the difference between the size of the star and the size of the chain becomes larger. For decreasing temperatures, the size of the stars lessens and a transition from the coiled state to that of the globule occurs. The size of the globule does not depend on the number of arms and is determined only by the total number of segments.

Limiting values of g at $T \rightarrow \infty$ are presented in Table 1. Also, there are presented values of g_{ph} for the phantom (ideal) star model [9], according to the expression $g_{\text{ph}} = (3f - 2)/f^2$, together with the results of our simulation. For the latter purpose, the distribution of the conformations Ω_n and the square radius of gyration $R_{I_n}^2$ over the number of intersections n and the corresponding average was determined according to the expression:

$$\langle R_I^2 \rangle_{\text{ph}} = \frac{\sum_{n=0}^{n_{\text{max}}} R_{I_n}^2 \Omega_n}{\sum_{n=0}^{n_{\text{max}}} \Omega_n}. \quad (6)$$

It is interesting to note that g -values for the athermal case with intersection avoidance appear to be in sufficiently fair agreement with those of phantom random progression cases. It could be affirmed that for stars with small number of arms ($f \leq 6$) the volume effects do not differ much from those of chains with the same total number of segments.

Fig. 5 presents temperature dependencies for the reduced modulus of the center of mass radius-vector R_c/N_{arm} . Its location was determined relative to the position of the star center, and was fixed as the coordinate's origin. For the chain ($f=2$), the dependency was

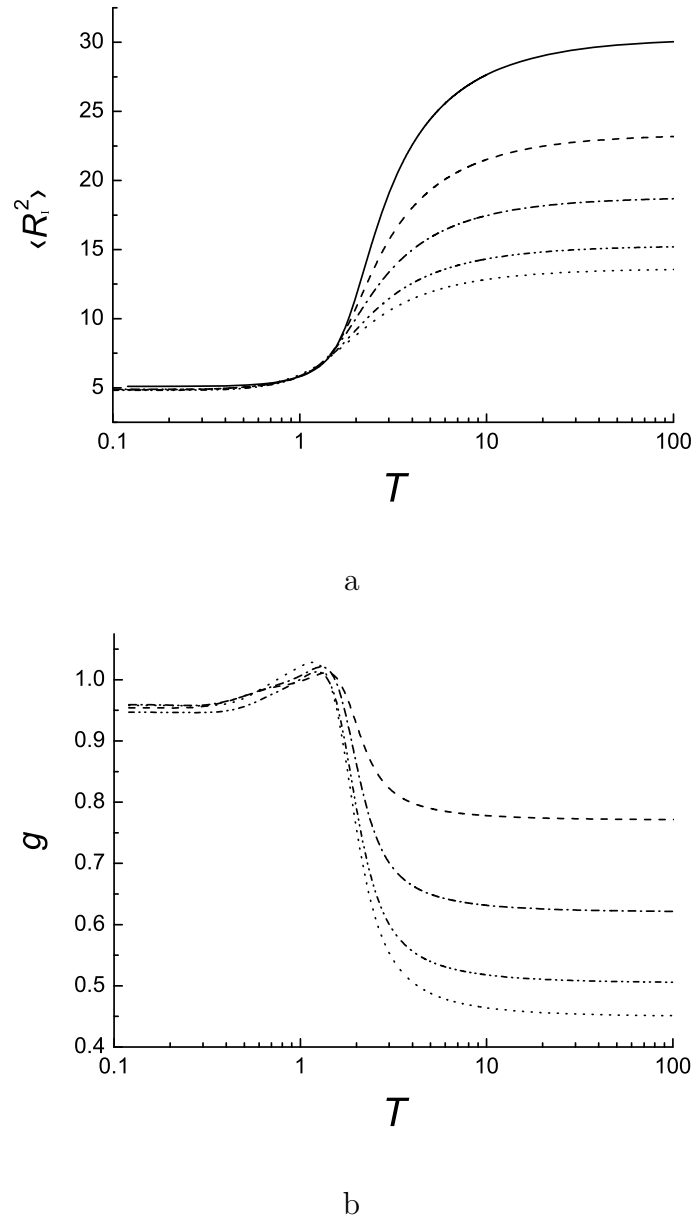


FIG. 4. Mean square radius of gyration (a) and g -factor (b) as functions of temperature for stars with different numbers of arms ($3 \div 6$). $N=70$ for $f=5$ and $N=72$ for all the rest. Legend, see in Fig. 2.

TABLE 1. Limiting values of the mean square radius of gyration $\langle R_I^2 \rangle$, and factor g for stars under athermal and ideal conditions.

f	$\lim_{T \rightarrow \infty} \langle R_I^2 \rangle$	g	$\langle R_I^2 \rangle_{\text{ph}}$	g_{ph}	g , ideal star [9]
2	29.1	1	13.4673	1	1
3	23.3474	0.8023	10.6939	0.7940	0.7778
4	18.7997	0.6460	8.7705	0.6512	0.625
5	15.2897	0.5254	7.2798	0.5406	0.52
6	13.6292	0.4684	6.5164	0.4839	0.4444

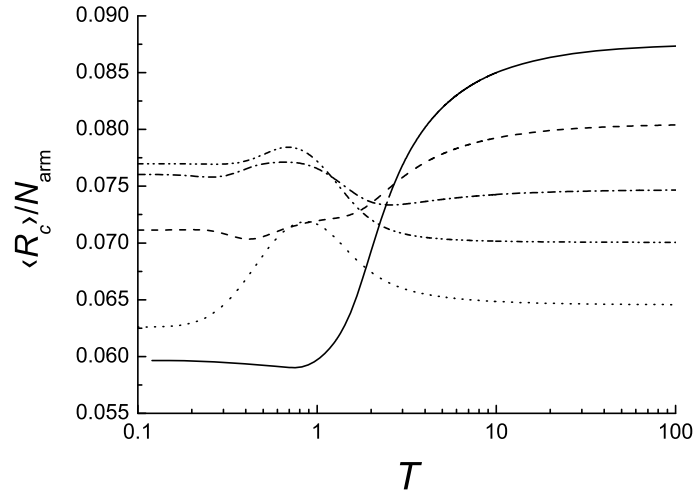


FIG. 5. Temperature dependence of the reduced modulus of the center of mass radius-vector R_c/N_{arm} for stars with different number of arms ($3 \div 6$). $N=70$ for $f=5$ and $N=72$ for all the rest. Legend, see in Fig. 2.

shown to increase. For stars with $f=4, 5, 6$, there exists a maximum that becomes more pronounced with an increased number of arms f . This might lead one to suppose that in the region of transition to the compact conformation, the internal state of the star is unstable, with its form essentially deviating from a symmetric one.

In order to analyze a star's form, it is necessary to calculate the orthogonal components of the square radius of gyration [23, 25]. First, all the components were obtained and then, matrix diagonalization was performed, such that the three nonzero components $L_1^2 < L_2^2 < L_3^2$, and that $R_1^2 = L_1^2 + L_2^2 + L_3^2$. These were initially averaged for each value of energy and finally, the canonical averages according to the relation (3) were obtained. All three components have different values, so we can state that the simulated stars have an average form of the three-axis ellipsoid. Knowledge of these components makes it possible to calculate the asphericity parameter of the star [11]:

$$\delta = 1 - 3(sf_1sf_2 + sf_2sf_3 + sf_3sf_1), \quad (7)$$

where the reduced components are $sf_1 = L_1^2/R_1^2$, $sf_2 = L_2^2/R_1^2$, $sf_3 = L_3^2/R_1^2$. The asphericity parameter ranges from 0 (absolute symmetry, sphere) up to 1 (the form of a rod). In the globular state, the star with any number of arms has a form similar to that of a sphere (Fig. 6a), and with elevated temperature, the asphericity increases. For the chain, this rising $\delta(T)$ is monotonous and for stars, this dependency has a maximum, which becomes more distinct with increased f . The maximum is slightly shifted to lower temperatures with increased f . Such a tendency can be explained in the following way: the greater the monomer density inside the star, the greater the relative asymmetry the star requires to attain a globular state. It is also clear from the figures that the greater the number of arms, the smaller the deviation of the star's form from an ideal sphere.

We have also considered the parameter that allows us to distinguish between the oblate and the elongated forms [11]

$$S^* = (3sf_1 - 1)(3sf_2 - 1)(3sf_3 - 1). \quad (8)$$

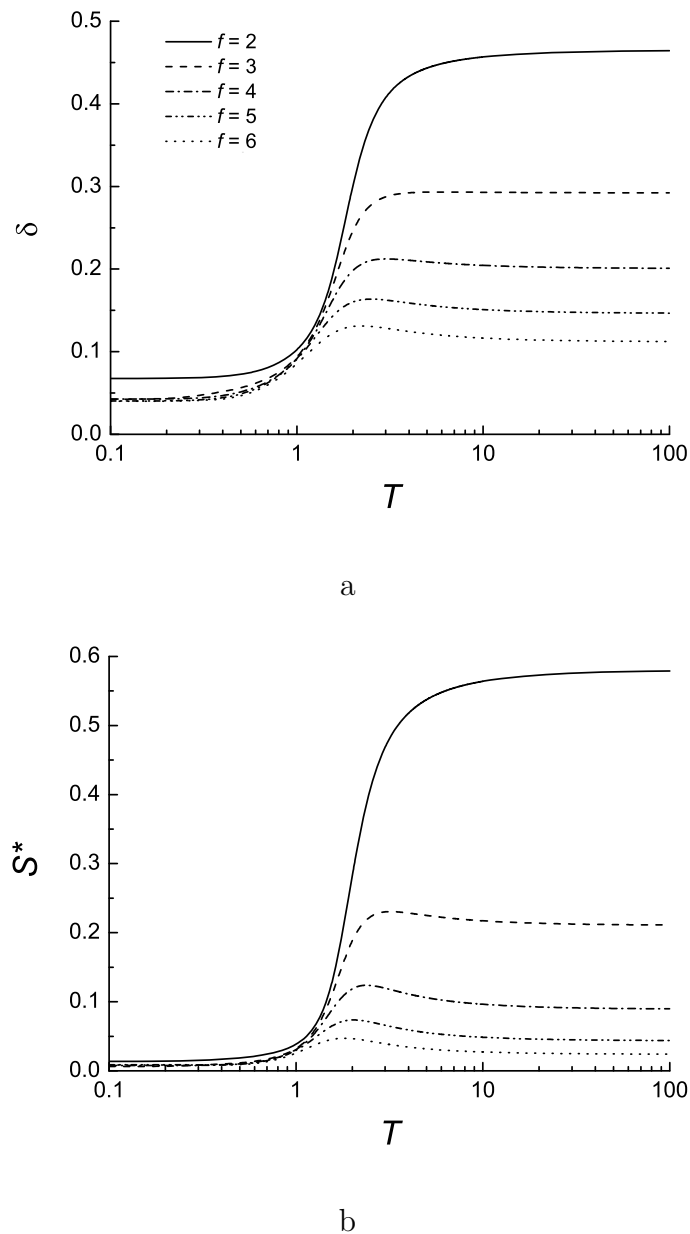


FIG. 6. Temperature dependence of the asphericity δ (a) and of the parameter S^* characterizing the form (b), for stars with different number of arms ($3 \div 6$). $N=70$ for $f=5$ and $N=72$ for all the rest.

This parameter ranges over the interval $[-0.25, 2]$, so it can be both negative (oblate form) and positive (elongated form). The temperature dependency of S^* is presented in Fig. 6b. It is seen that $S^* > 0$ over the entire temperature range, and hence, the star has the average form of a slightly elongated sphere. It is also worth noting that there is a temperature for which the elongation for stars has a slight maximum while for a chain, the dependency $S^*(T)$ is monotonous. With the transition to the globular state ($T < 1$), the elongation vanishes.

Fig. 7 presents the dependencies $\delta(T)$, $S^*(T)$ for 6-arm stars with different arm lengths. Increasing the arms' length was shown to shift the maxima of δ and S^* to higher temperatures and make it slightly more narrow.

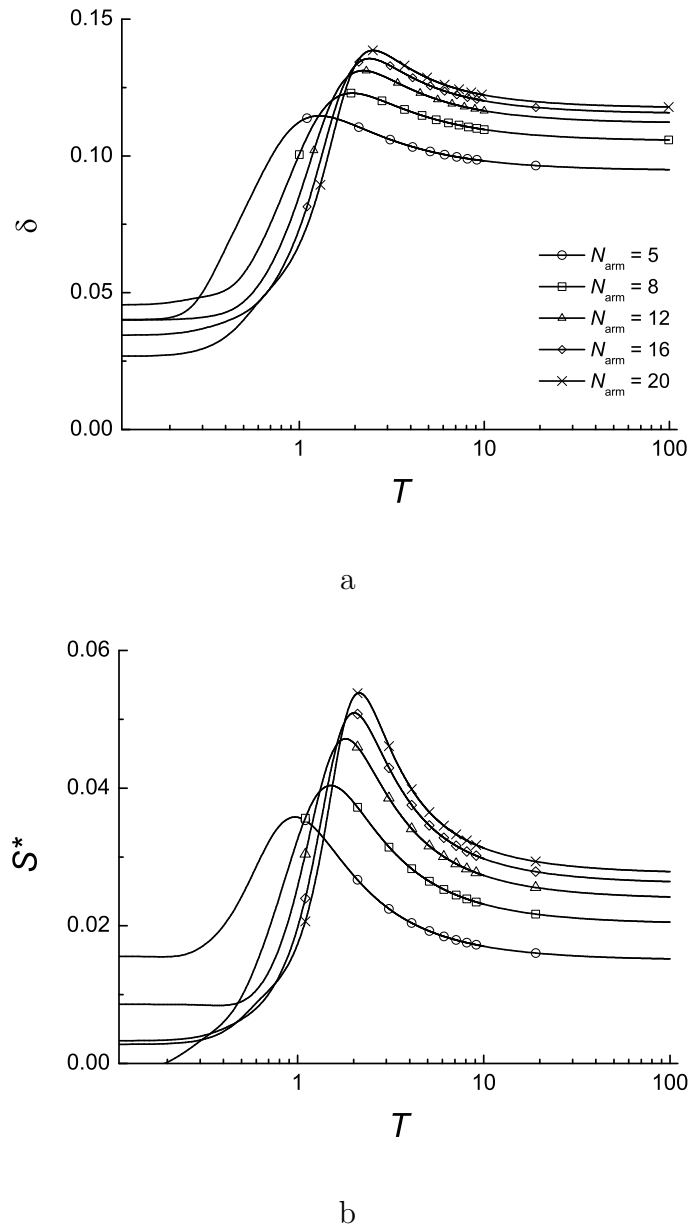


FIG. 7. Temperature dependencies of the asphericity δ (a) and of the parameter S^* characterizing the form (b), for five 6-arm stars with varying arm lengths ($N_{\text{arm}}=5, 8, 12, 16, 20$). Symbols in lines are used for marking different lines.

5. Conclusion

In this paper, we have studied a lattice model of regular, non-charged star polymer with the attractive interactions between segments and with varying number of arms. The effect of these characteristics upon temperature behavior of structural characteristics for star polymers is demonstrated. Using the entropic sampling method [18], we could calculate structural properties for stars over a wide temperature range and show that at certain temperatures, a transition of the coil-globule type occurs. This transition shifts to lower temperatures with an increased number of the arms, since it is more difficult to collapse

stars with greater number of arms into a compact globule. In the area of this transition, the form of the star becomes most asymmetric i. e. an elongated ellipsoid.

The number of segments in the considered stars was not very large, however the applied method provides an opportunity to increase this value. Moreover, the next step of this work can imply simulation of star polymers where electrostatic interactions are considered.

References

- [1] Rud O. V., Mercurieva A. A., Leermakers F. A. M., and Birshtein T. M. Collapse of polyelectrolyte star. Theory and modeling. *Macromolecules*, 2012, **45**, P. 2145–2160.
- [2] Muzafarov A., Vasilenko N., Tatarinova E., Ignateva G., Myakushev V., Obrezkova M., Meshkov I., Voronina N., Novozhilova O. Macromolecular nanoobjects — promising area of polymer chemistry. *Macromolecular compounds C.*, 2011, **53**(7), P. 1217–1230 (in Russian).
- [3] Likos C. N. Soft matter with soft particles. *Soft Matter.*, 2006, **2**, P. 478–498.
- [4] Wang Z., He X. Phase transition of a single star polymer: a Wang-Landau sampling study. *J. Chem. Phys.*, 2011, **135**, P. 094902.
- [5] Polotsky A. A., Zhulina E. B., Birshtein T. M. Effect of the ionic strength on collapse transition in star-like polyelectrolytes. *Macromol. Symp.*, 2009, **278**, P. 24–31.
- [6] Alhoranta A. M., Lehtinen J. K., Urtti A. O., Butcher S. J., Aseyev V. O., Tenhu H. J. Cationic amphiphilic star and linear block copolymers: synthesis, self-assembly, and in vitro gene transfection. *Biomacromolecules*, 2011, **12**, P. 3213–3222.
- [7] Aryal S., Prabakaran M., Pilla S., Gong S. Biodegradable and biocompatible multi-arm star amphiphilic block copolymer as a carrier for hydrophobic drug delivery. *International Journal of Biomacromolecules*, 2009, **44**, P. 346.
- [8] Cameron D., Shaver M. Aliphatic polyester polymer stars: synthesis, properties and applications in biomedicine and nanotechnology. *Chemical Society Reviews*, 2011, **40**, P. 1761–1776.
- [9] Grossberg A. Y., Khokhlov A. R. *Statistical physics of macromolecules*. Moscow, Nauka, 1989 (in Russian).
- [10] Clisby N. Efficient implementation of the pivot algorithm for self-avoiding walks. *J. Stat. Phys.*, 2010, **140**, P. 349–392.
- [11] Zifferer G., Eggerstorfer D. Monte Carlo simulation studies of the size and shape of linear and star-branched copolymers embedded in a tetrahedral lattice. *Macromol. Theory. Simul.*, 2010, **19**, P. 458–482.
- [12] Wüst T., Lee Yu., Landau D. Unraveling the beautiful complexity of simple lattice model polymers and proteins using Wang-Landau sampling. *J. Stat. Phys.*, 2011, **144**, P. 638–651.
- [13] Yurchenko A. A., Antyukhova M. A., Vorontsov-Velyaminov P. N. Investigation of the interaction of the polymer with the surface by entropic modeling. *J. Structure Chemistry.*, 2011, **52**(6), P. 1216–1223 (in Russian).
- [14] Vogel T., Bachmann M., and Janke W. Freezing and collapse of flexible polymers on regular lattices in three dimensions. *Phys. Rev. E.*, 2007, **76**, P. 061803.
- [15] Volkov N. A., Yurchenko A. A., Lyubartsev A. P., Vorontsov-Velyaminov P. N. Entropic sampling of free and ring polymer chains. *Macromol. Theory Simul.*, 2005, **14**, P. 491–504.
- [16] Berg B. A., Neuhaus T. Multicanonical ensemble: a new approach to simulate first-order phase transitions. *Phys. Rev. Lett.*, 1992, **68**, P. 9–12.
- [17] Lee J. New Monte Carlo algorithm: entropic sampling. *Phys. Rev. Lett.*, 1993, **71**, P. 211–214.
- [18] Wang F., Landau D. P. Efficient, multiple-range random walk algorithm to calculate the density of states. *Phys. Rev. Lett.*, 2001, **86**, P. 2050–2035.
- [19] Vorontsov-Velyaminov P. N., Yurchenko A. A., Antyukhova M. A., Silantyeva I. A., Antipina A. Yu. Entropic sampling of polymers: A chain near a wall, polyelectrolytes, star-shaped polymers. *Polymer Science C*, 2013, **55**(1), P. 112–124.
- [20] Silantyeva I. A., Vorontsov-Velyaminov P. N. Thermodynamic properties of star shaped polymers investigated with Wang-Landau Monte Carlo simulations. *Macromol. Symp.*, 2012, **317-318**, P. 267–275.
- [21] Silantyeva I. A., Vorontsov-Velyaminov P. N. The calculation of the density of states and the thermal properties of the polymer chains and stars on a lattice by Monte Carlo method using the Wang-Landau algorithm. *Numerical Methods and Programming*, 2011, **12**, P. 397–408 (in Russian).
- [22] Seaton D. T., Wüst T., Landau D. P. Collapse transition in a flexible homopolymer chain: application of the Wang-Landau algorithm. *Phys. Rev. E.*, 2010, **81**, P. 011802.

- [23] Martemyanova J. A., Stukan M. R., Ivanov V. A., Müller M., Paul W., Binder K. Dense orientationally ordered states of a single semiflexible macromolecule: An expanded ensemble Monte Carlo simulation. *J. Chem. Phys.*, 2005, **122**, P. 174907.
- [24] 24. Wang Z., Wang L., Chen Y., He X. Phase transition behaviours of a single dendritic polymer. *Soft Matter.*, 2014, **10**, P. 4142–4150.
- [25] 25. Arkin H., Janke W. Ground-State properties of a polymer chain in attractive sphere. *J. Phys. Chem. B.*, 2012, **116**, P. 10379–10386.